

Preparation, characterization, and electrocatalytic properties of hybrid coatings of hexacyanometalate-doped-cationic films

Shen-Ming Chen · Wen-Yan Chzo · R. Thangamuthu

Received: 30 September 2007 / Revised: 17 November 2007 / Accepted: 30 November 2007 / Published online: 15 January 2008
© Springer-Verlag 2007

Abstract Electrochemically active hybrid coatings based on cationic films, didodecyldimethylammonium bromide (DDAB), and poly(diallyldimethylammonium chloride) (PDDAC) are prepared on electrode surface by cycling the film-covered electrode repetitively in a pH 6.5 solution containing $\text{Fe}(\text{CN})_6^{3-}$ and $\text{Ru}(\text{CN})_6^{4-}$ anions. Modified electrodes exhibited stable and reversible voltammetric responses corresponding to characteristics of $\text{Fe}(\text{CN})_6^{3-/4-}$ and $\text{Ru}(\text{CN})_6^{4-/3-}$ redox couples. The cyclic voltammetric features of hybrid coatings resemble that of electron transfer process of surface-confined redox couple. Electrochemical quartz crystal microbalance results show that more amounts of electroactive anionic complexes partitioned into DDAB coating than those doped into PDDAC coating from the same doping solution. Peak potentials of hybrid film-bound redox couples showed a negative shift compared to those at bare electrode and this shift was more pronounced in the case of DDAB. Finally, the advantages of hybrid coatings in electrocatalysis are demonstrated with sulfur oxoanions.

Keywords Hybrid coatings · Simultaneous doping · Modified electrode · DDAB · PDDAC · Electrocatalysis · Sulfur oxoanions

Introduction

Modification of electrode surfaces with electroactive films has been the active area of research during past three

decades mainly due to their many potential applications in widely differing areas like energy conversion and storage, electrocatalysis, electroanalysis, electrochromism, molecular electronics, biosensor, and media for controlled drug release [1–4]. In particular, potential applications of such electroactive coatings in understanding the mechanism of electron transfer reactions in complex biological systems, such as enzymes and antibodies, and catalysis of electrochemical reactions have provided much of the incentive for this development [1–8]. In view of the enormous practical and fundamental interest of the subject, chemically modified electrodes is still one of the active areas of research.

Among the materials used to fabricate electroactive coating on electrode surfaces, ionomer membranes, with ionizable groups attached to organic polymer backbones, is attractive in many aspects. The use of ionomers for surface modification has grown in popularity ever since Oyama and Anson [9] demonstrated the binding of counterionic reactants to poly(4-vinylpyridine) (PVP) film on the electrode surface. In acidic medium, the protonated PVP coating extracts the anionic complexes like ferrocyanide and hexachloroiridate from the contacting solution by ion-exchange process. Similarly, Du Pont's Nafion membrane has been used to immobilize the cationic reactants on the electrode surfaces [3]. Because this is simple means to immobilize electroactive species to the electrode surface, later this approach extended to similar materials.

Kunitake et al. [10, 11] first incorporated iron heme proteins into vesicles and multilayer films of insoluble surfactants, and this work paved the way to explore electrochemistry of films of complex biological macromolecules such as proteins and surfactants or lipids on electrodes [12–19]. Rusling et al. [13] has found that inclusion of myoglobin (Mb) in films of cationic surfactants, didodecyldimethyl ammonium bromide (DDAB), on pyrolytic graphite (PG), or glassy carbon

S.-M. Chen (✉) · W.-Y. Chzo · R. Thangamuthu
Department of Chemical Engineering and Biotechnology,
National Taipei University of Technology,
No. 1, Section 3, Chung-Hsiao East Road,
Taipei, Taiwan 106, Republic of China
e-mail: smchen78@ms15.hinet.net

(GC) led to electron transfer rates up to 1,000 times higher than that between bare electrodes and Mb in solution. The substantial enhancement in electron transfer rate was attributed to the favorable orientation of Mb in the films and, most importantly, to the adsorption of surfactant at the film-electrode interface, which prevents the adsorption-induced passivation. The stability of didodecyldimethylammonium bromide (DDAB) coating was improved when coating as composite films by mixing with ionomers like Nafion [20] and Eastman AQ [21]. Similar kind of coatings were prepared from poly(dimethyldiallylammonium) chloride (PDDAC) and then concerted into water-insoluble network by gamma irradiation [22–24].

In the present investigation, stable hybrid films based on DDAB and PDDAC are prepared by incorporating hexacyanometalates. The electrochemical properties of both coatings were compared. Finally, the electrocatalytic behavior of hexacyanometalate-doped PDDAC-modified electrodes was tested toward sulfur oxoanions.

Experimental

Didodecyldimethylammonium bromide, poly(diallyldimethylammonium chloride), $K_4[Fe(CN)_6] \cdot 3H_2O$, and $K_4[Ru(CN)_6] \cdot xH_2O$ were obtained from Aldrich and were used as received. All other chemicals used were of analytical grade and used without further purification. Generally, all the electrochemical experiments were carried out using pH 6.5 phosphate buffer solutions. For pH variation study, solutions of different pH values varying from 1 to 8 were prepared from 0.1 M NaCl. Aqueous solutions were prepared using doubly distilled deionized water and high purity nitrogen gas was used to deaerate as well as flow over the solutions during experiments. All the measurements were carried out at room temperature.

The electrochemical experiments were carried out with Bioanalytical system (Model CV-50W) and CH Instruments (Model CHI-400). Cyclic voltammograms were recorded in a three-electrode cell configuration, in which a BAS glassy carbon electrode (area=0.07 cm²) was used as working electrode. The auxiliary compartment contained a platinum wire that was separated by a medium-sized glass frit. All cell potentials were recorded using Ag|AgCl|KCl(sat) reference electrode. The working electrode for the electrochemical quartz crystal microbalance (EQCM) measurements was an 8-MHz AT-cut quartz crystal with gold coating (5 mm diameter).

DDAB (or PDDAC) film-modified electrode was prepared as follows. First, measured aliquots of DDAB (or PDDAC) solution was used to cover the pretreated electrode surface and then dried in warm flow of air (at about 50 °C) from 10 cm away from electrode surface and formed a film on it. Hexacyanometalate-doped DDAB (or

PDDAC) film-modified electrodes were prepared by cycling the potential of respective film-coated electrodes at a scan rate of 100 mV s⁻¹ between a desired potential range in pH 6.5 buffer solution containing Fe(CN)₆³⁻ (or Ru(CN)₆³⁻, or both). Prior to modification, glassy carbon electrode was polished with 0.05 μm alumina on Buehler felt pads and then ultrasonically cleaned for about a minute in water. After film formation, the electrode was rinsed with distilled water and used for further characterization.

Results and discussion

Preparation of hexacyanometalate-doped DDAB film-modified electrodes

Figure 1a shows a series of cyclic voltammograms obtained in pH 6.5 phosphate buffer solution containing 1×10^{-4} M Fe(CN)₆³⁻ with DDAB film-coated GC electrode. The peak current continues to increase as the electrode is cycled continuously between +0.4 and -0.3 V, which suggests that more and more Fe(CN)₆³⁻ is extracted from the solution by

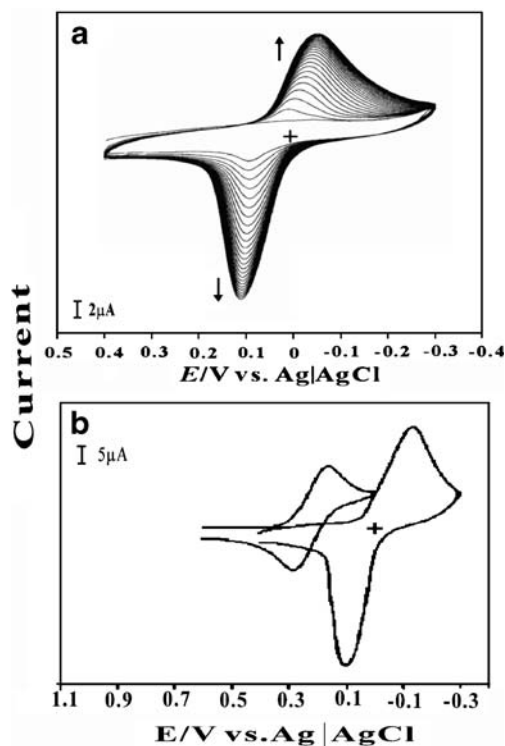


Fig. 1 **a** Consecutive voltammetric curves obtained with DDAB film modified glassy carbon electrode recorded at 0.1 V s⁻¹ between +0.4 and -0.3 V in a pH 6.5 phosphate buffer solution containing 1×10^{-4} M Fe(CN)₆³⁻. The arrows indicate the change in the voltammetric peaks with increasing scan numbers. **b** Cyclic voltammogram of: **a** Fe(CN)₆³⁻-doped DDAB film-modified GCE in pH 6.5 phosphate buffer and **b** 1×10^{-4} M Fe(CN)₆³⁻ at bare GCE in pH 6.5 phosphate buffer solution. Scan rate = 0.1 V s⁻¹

the cationic coating. After about 30 repetitive cycles, concentration of $\text{Fe}(\text{CN})_6^{3-}$ in the film reached a steady state, and peak currents did not increase further. It is appropriate to mention at this stage that this steady-state condition was used for most of characterization studies. The successive voltammograms in the figure show how the peak potentials shift as more $\text{Fe}(\text{CN})_6^{3-}$ enter the coating. The shift is more pronounced in the case of cathodic peak compared to anodic. Also, the peak width was smaller for anodic than for cathodic scans as observed by Rusling and Zhang [25].

Curve a' of Fig. 1b shows cyclic voltammogram of $\text{Fe}(\text{CN})_6^{3-/4-}$ redox couple confined to the electrode surface within the DDAB film in pure supporting electrolyte. The formal potential of the $\text{Fe}(\text{CN})_6^{3-/4-}$ within the film, obtained as $(E_{\text{pa}} + E_{\text{pc}})/2$ (where E_{pa} and E_{pc} are the anodic and cathodic peak potentials, respectively), is 0.03 V. This value is less positive than that of the molecular analog dissolved in solution (curve b' of Fig. 1b). Similar behavior was reported in [25] for the same surfactant film-modified electrode but with different supporting electrolyte. Such potential shifts have been noticed by other [25–28] for $\text{Fe}(\text{CN})_6^{3-/4-}$ redox couple confined to polymer film. It is an indication that the environment in film is different from solution for $\text{Fe}(\text{CN})_6^{3-/4-}$ redox couple. The shift in the formal potential suggests that factors other than simple electrostatic interactions between DDAB coating and incorporated anions must be involved. Note that, in Fig. 1b, peak currents of modified electrode are larger than those at bare electrode in the same loading solution because a large number of electroactive ions may be bound in the DDAB film.

Similarly, $\text{Ru}(\text{CN})_6^{4-}$ was incorporated into DDAB film by repetitive cycling of film-covered electrode in 1×10^{-4} M $\text{Ru}(\text{CN})_6^{4-}$ solution. The electrode was cycled between +0.3 and 0.8 V at a scan rate of 0.1 V s^{-1} and results are presented in Fig. 2a. If one looks at cyclic voltammograms presented in Fig. 2a and b, it can be realized that $\text{Ru}(\text{CN})_6^{4-/3-}$ redox couple confined in the coating showed similar behaviors as that of $\text{Fe}(\text{CN})_6^{3-/4-}$: (1) the width of anodic peak was smaller and its current value is also lower compared to relatively sharp peak of cathodic scans; (2) peak currents of modified electrode are larger than those at bare electrode. Thus, it can be concluded that the environment in the film is different from the solution for both $\text{Fe}(\text{CN})_6^{3-/4-}$ and $\text{Ru}(\text{CN})_6^{4-/3-}$ redox couples.

Electrochemical properties of hexacyanometalate-doped DDAB film-modified electrodes

Figure 3a shows cyclic voltammograms of $\text{Fe}(\text{CN})_6^{3-}$ -doped DDAB film-modified electrode in pH 6.5 phosphate

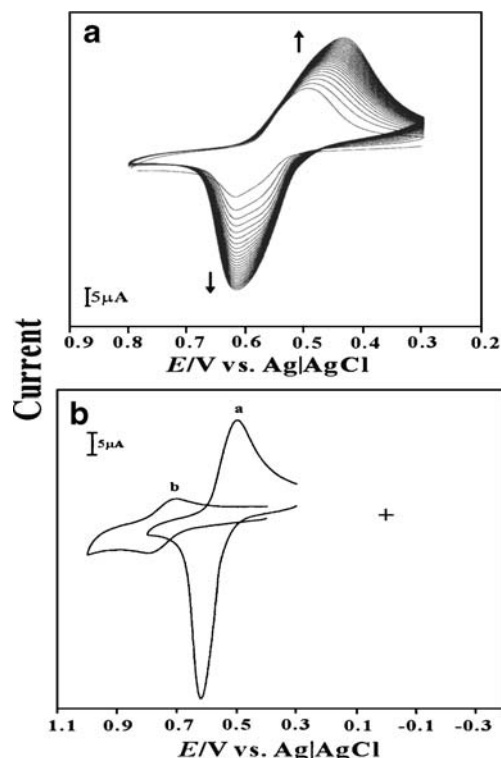


Fig. 2 a Consecutive voltammograms obtained with DDAB film modified glassy carbon electrode recorded at 0.1 V s^{-1} between +0.3 and +0.8 V in a pH 6.5 phosphate buffer solution containing 1×10^{-4} M $\text{Ru}(\text{CN})_6^{4-}$. b Cyclic voltammogram of: a $\text{Ru}(\text{CN})_6^{4-}$ -doped DDAB film-modified GCE in pH 6.5 phosphate buffer, and b 1×10^{-4} M $\text{Ru}(\text{CN})_6^{4-}$ at bare GCE in pH 6.5 phosphate buffer solution. Scan rate = 0.1 V s^{-1}

buffer solution at different scan rates. Both anodic and cathodic currents increase linearly with scan rates up to 200 mVs^{-1} , as shown in the inset, in accord with the equation for ideal, one-electron, reversible thin-layer electrochemistry [3]

$$i_p = F^2 A \Gamma_0 \nu / 4RT \quad (1)$$

where F is Faraday's constant, A is area of the electrode, Γ_0 is surface concentration of the electroactive species, and R is the gas constant. However, the peak shapes were non-ideal, also peak-to-peak separation (ΔE_p) is not zero and its value increases with scan rate. Similar voltammetric characteristics were obtained with $\text{Ru}(\text{CN})_6^{4-}$ -doped DDAB film-modified electrode when cycled in pH 6.5 phosphate buffer solution at different scan rates (Fig. 3b).

The electrochemical response of hexacyanometalate-doped DDAB film-coated electrodes in 0.1 M NaCl solutions of different pH were investigated using cyclic voltammetric technique. Peak potentials were nearly independent at higher pH values (not shown). However, our modified

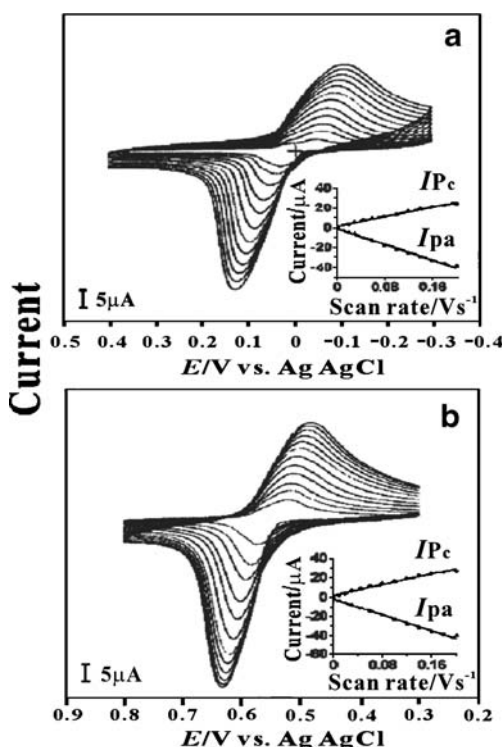


Fig. 3 **a** Cyclic voltammograms obtained with $\text{Fe}(\text{CN})_6^{3-}$ -doped DDAB film-modified glassy carbon electrode in pH 6.5 phosphate buffer solution at different scan rates. The inset shows plot of anodic and cathodic peak currents vs. scan rates. **b** Cyclic voltammograms obtained with $\text{Ru}(\text{CN})_6^{4-}$ -doped DDAB film-modified glassy carbon electrode in pH 6.5 phosphate buffer solution at different scan rates. The inset shows plot of anodic and cathodic peak currents vs. scan rates

electrodes exhibited pH dependent voltammetric peak potentials (i.e., the anodic and cathodic peak potentials of the modified electrode were shifted to a less positive value with increasing pH of the contacting solution) at lower pH as shown in Fig. 4. The $E_{1/2}$ vs. pH plots yields straight line as shown in the insets.

Simultaneous incorporation of hexacyanometalates into cationic coatings

In a further step, we are interested in preparing hybrid coatings on electrode surfaces by simultaneous doping of multiple-charged anionic complexes into cationic films for both fundamental as well as catalytic applications. In the present investigation, $\text{Fe}(\text{CN})_6^{3-}$ and $\text{Ru}(\text{CN})_6^{4-}$ complexes were doped into cationic films such as DDAB and PDDAC, and the resulting hybrid coatings were studied as model systems. Since the redox potentials of these two anionic complexes are well separated, they were chosen so that the electrochemical responses of both redox couples in the coatings could be observed and used to mediate electrochemical reaction of two analytes using the same coating.

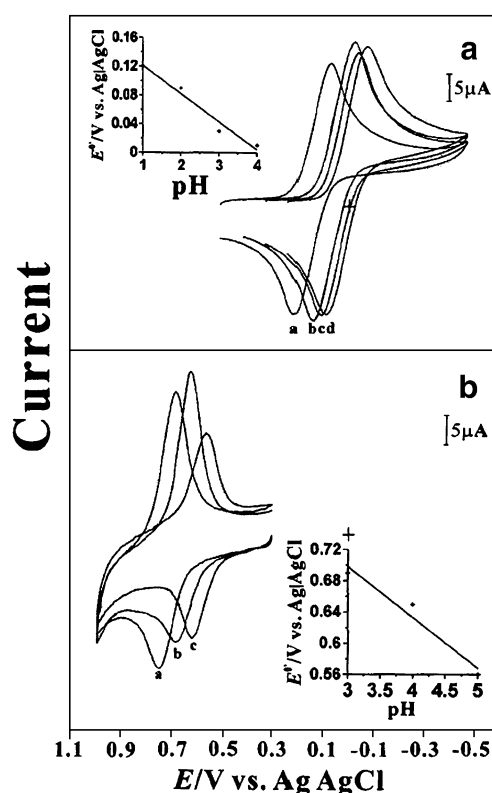


Fig. 4 Cyclic voltammograms of: **a** $\text{Fe}(\text{CN})_6^{3-}$ -doped DDAB film-modified GCE and **b** $\text{Ru}(\text{CN})_6^{4-}$ -doped DDAB film-modified GCE in 0.1 M NaCl solutions of different pH. The insets show a plot of formal potential vs. pH. Scan rate=0.1 V/s

DDAB coating

Figure 5 shows a series of cyclic voltammograms obtained with DDAB film-coated GC electrode in pH 6.5 phosphate buffer solution containing 5×10^{-4} M of $\text{Fe}(\text{CN})_6^{3-}$ and $\text{Ru}(\text{CN})_6^{4-}$. The voltammograms exhibited two reversible redox couples corresponding to $\text{Fe}(\text{CN})_6^{3-/4-}$ and $\text{Ru}(\text{CN})_6^{4-/3-}$ redox reactions. The results show that cationic DDAB coatings capable of incorporating two different multiple-charged anionic complexes simultaneously. The formal potentials of the complexes in the coating were shifted to more negative potentials when compared to their values at bare electrode (curve b' of Fig. 5). It should be remembered that similar pattern was observed when individual complex incorporated into DDAB coating, as discussed in "Preparation of hexacyanometalate-doped DDAB film-modified electrodes." The other characteristics, such as peak shape ΔE_p , and were also found to be following similar trend. The results showed that the environment in film is different from solution for both $\text{Fe}(\text{CN})_6^{3-/4-}$ and $\text{Ru}(\text{CN})_6^{4-/3-}$ redox couples but the influence of one on other complex in the coating is not significant.

Figure 6 shows cyclic voltammograms of hybrid film at different scan rates after transferring to pH 6.5 phosphate

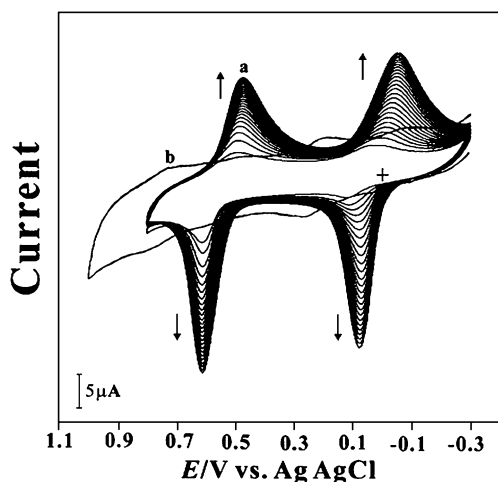


Fig. 5 *a* Consecutive voltammetric curves obtained with DDAB film modified GCE in a pH 6.5 phosphate buffer solution containing 5×10^{-4} M $\text{Fe}(\text{CN})_6^{3-}$ and 5×10^{-4} M $\text{Ru}(\text{CN})_6^{4-}$ and *b* cyclic voltammograms of bare GCE in a pH 6.5 phosphate buffer solution containing 5×10^{-4} M $\text{Fe}(\text{CN})_6^{3-}$ and 5×10^{-4} M $\text{Ru}(\text{CN})_6^{4-}$. Scan rate = 0.1 V s^{-1}

buffer solution. The presence of two chemically reversible redox couples indicates that DDAB film could retain both anions firmly by electrostatic interaction. The anodic and cathodic peak currents of complexes increase linearly with scan rates, as shown in insets. This shows that the hybrid film is stable and consistent with a diffusionless, reversible electron transfer process.

PDDAC coating

Figure 7a illustrates simultaneous incorporation of $\text{Fe}(\text{CN})_6^{3-}$ and $\text{Ru}(\text{CN})_6^{4-}$ anions into PDDAC coating during repetitive cycling of PDDAC-coated electrode between -0.2 and $+1.2$ V in pH 6.5 phosphate buffer solution containing 5×10^{-4} M of $\text{Fe}(\text{CN})_6^{3-}$ and $\text{Ru}(\text{CN})_6^{4-}$. The growth of cyclic voltammetric peak currents indicates that two redox couple with formal potentials of about 0.22

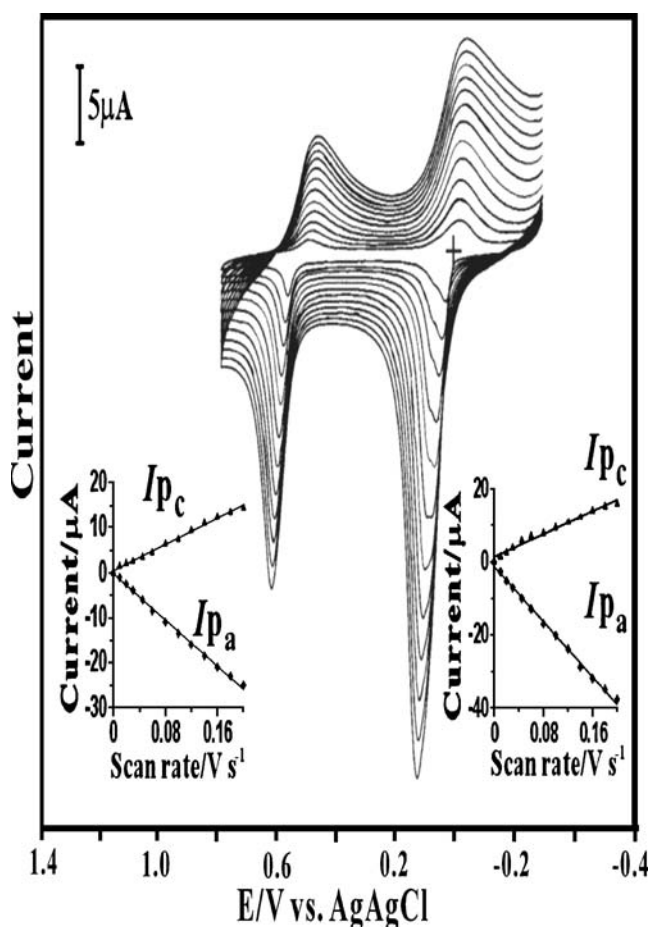


Fig. 6 Cyclic voltammograms obtained with $\text{Fe}(\text{CN})_6^{3-}$ as well as $\text{Ru}(\text{CN})_6^{4-}$ simultaneously doped DDAB film-modified glassy carbon electrode in pH 6.5 phosphate buffer solution at different scan rates. The insets show plots of anodic and cathodic peak currents vs. scan rates

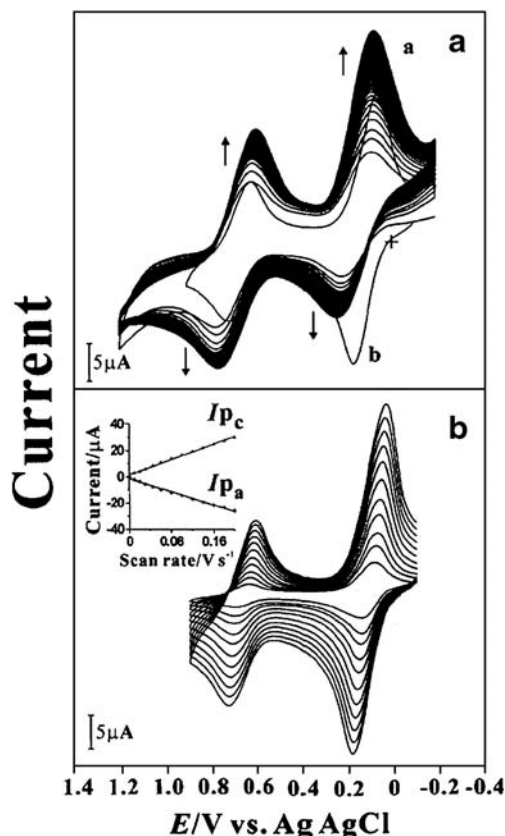


Fig. 7 *a* Consecutive voltammetric curves obtained with PDDAC film-modified GCE in a pH 6.5 phosphate buffer solution containing 5×10^{-4} M $\text{Fe}(\text{CN})_6^{3-}$ and 5×10^{-4} M $\text{Ru}(\text{CN})_6^{4-}$ and *b* cyclic voltammograms of bare GCE in a pH 6.5 phosphate buffer solution containing 5×10^{-4} M $\text{Fe}(\text{CN})_6^{3-}$ and 5×10^{-4} M $\text{Ru}(\text{CN})_6^{4-}$. Scan rate = 0.1 V s^{-1} . **b** Cyclic voltammograms obtained with $\text{Fe}(\text{CN})_6^{3-}$ as well as $\text{Ru}(\text{CN})_6^{4-}$ simultaneously doped PDDAC film-modified glassy carbon electrode in pH 6.5 phosphate buffer solution at different scan rates. The insets show plots of anodic and cathodic peak currents vs. scan rates

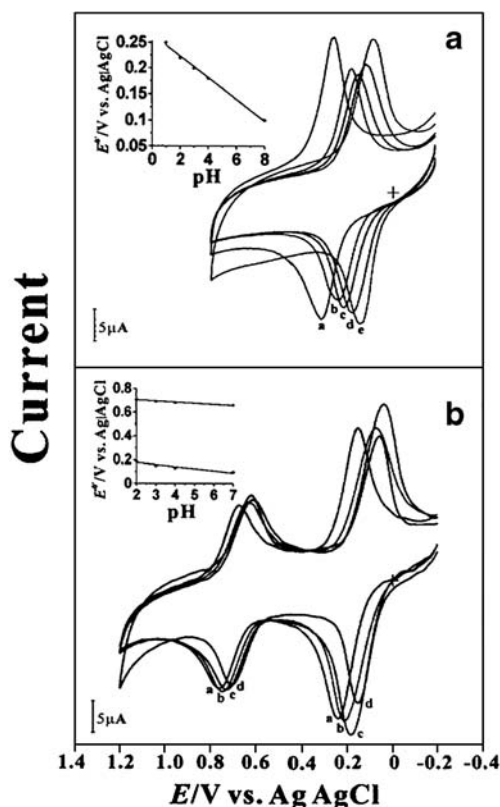


Fig. 8 Cyclic voltammograms obtained from 0.1 M NaCl solutions of different pH: **a** for Fe(CN)₆^{3-/4-}-doped PDDAC film-modified GCE and **b** for Fe(CN)₆^{3-/4-} as well as Ru(CN)₆^{4-/3-} simultaneously doped PDDAC film-modified GCE. The insets show a plot of formal potential vs. pH. Scan rate=0.1 V s⁻¹

and 0.74 V (which are corresponding to Fe(CN)₆^{3-/4-} and Ru(CN)₆^{4-/3-} redox couples) coexisted in the PDDAC coating. As found in DDAB film, the peak currents of PDDAC hybrid film are larger compared to those at bare electrode, as shown in curve b. However, the difference is

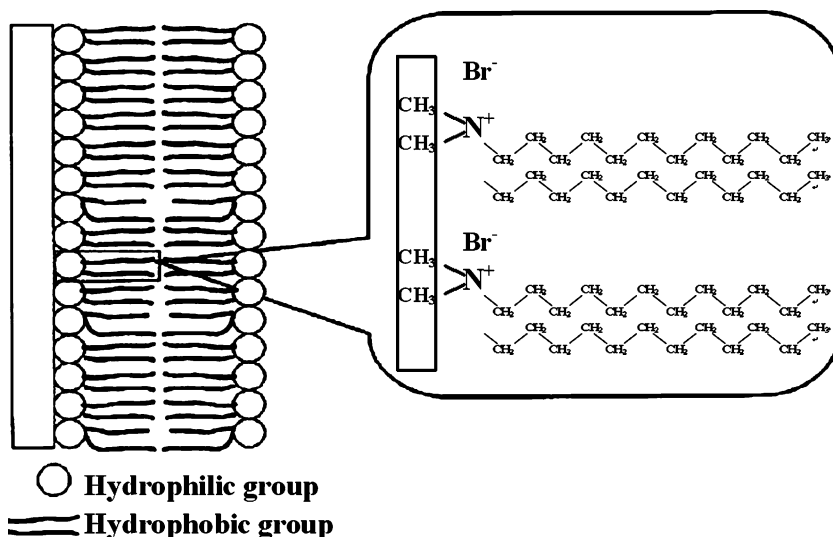
lower in the case of PDDAC-based hybrid film. Heineman et al. [24] have reported that 34-fold increase in peak current for Fe(CN)₆⁴⁻-doped gamma-irradiated PDDAC film-coated electrode than those obtained at bare graphite electrode. The magnitude of increase varies depending on the film thickness and/or supporting electrolyte [22, 23]. They also noticed negative shift in formal potential with PDDAC film electrodes [24, 29] as in the present investigation.

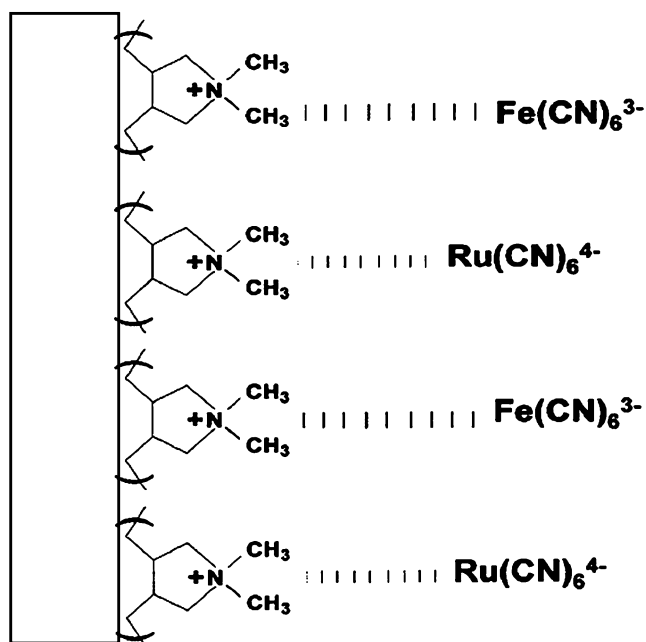
Figure 7b demonstrates cyclic voltammetric response of PDDAC film-confined Fe(CN)₆^{3-/4-} and Ru(CN)₆^{4-/3-} redox couples at different scan rates when the modified electrode scanned in pure buffer solution. The results showed that redox couples in the hybrid coating were stable and electrochemically active in Fe(CN)₆^{3-/4-}, Ru(CN)₆^{4-/3-}, and PDDAC-free buffer solution. The linear response shown in the inset is in consistent with a diffusionless, reversible electron transfer process. The pH dependence voltammetric responses of Fe(CN)₆^{3-/4-}-doped-PDDAC film as well as hybrid PDDAC film containing Fe(CN)₆³⁻ and Ru(CN)₆⁴⁻ redox couples were shown in Fig. 8a and b, respectively. The formal potential of both films are found to move towards more negative potential with increasing pH of contacting solution in the pH range 1 to 5.

Comparison of hybrid coatings derived from DDAB and PDDAC

It is interesting to compare the properties of hybrid films derived from DDAB and PDDAC in order to utilize them in understanding mechanism of electron transfer reactions in complex biological macromolecules and possible applications of these assemblies in electrocatalysis and sensors. Schemes 1 and 2 illustrate DDAB film on electrode

Scheme 1 Schematic illustration of DDAB film on the electrode surface





Scheme 2 Schematic illustration of electrostatic interaction between $\text{Fe}(\text{CN})_6^{3-}$ and $\text{Ru}(\text{CN})_6^{4-}$ anions, and PDDAC film

surface and electrostatic interaction between the $\text{Fe}(\text{CN})_6^{3-}$ and $\text{Ru}(\text{CN})_6^{4-}$ anions, and the PDDAC film, respectively. As shown, DDAB self-assembled film formed on the electrode surface. Because these films are positively charged, anionic complexes were extracted from contacting solution and firmly held in the film due to electrostatic interaction between anions and cationic coatings as illustrated in Scheme 2. This phenomenon was well demonstrated by DDAB and PDDAC coatings, as shown in Figs. 5 and 7. Continuous increase in peak currents indicates that more amounts of both anions entered into the coatings. However, it can be noticed from the peak current values that the doping is somewhat systematic in DDAB coating in comparison with PDDAC film. In other words, more amounts of anions doped into DDAB film and/or PDDAC film saturated with anionic complexes quickly. In order to validate our assumption, simultaneous EQCM and cyclic voltammetric measurements were carried out to follow the doping of $\text{Fe}(\text{CN})_6^{3-}$ into DDAB and PDDAC film (Fig. 9a and b). EQCM results show that during the first ten cyclic voltammetric scans, about 4570 ng/cm^2 of $\text{Fe}(\text{CN})_6^{3-}$ was deposited into DDAB coating, while 1930 ng/cm^2 of $\text{Fe}(\text{CN})_6^{3-}$ was doped into PDDAC coating during the first nine scans. Moreover, the difference in the peak currents between modified electrode and the bare electrode was substantially higher in DDAB-compared to PDDAC-film-covered electrode. Thus, more amount of catalyst could be doped into DDAB compared to PDDAC coating.

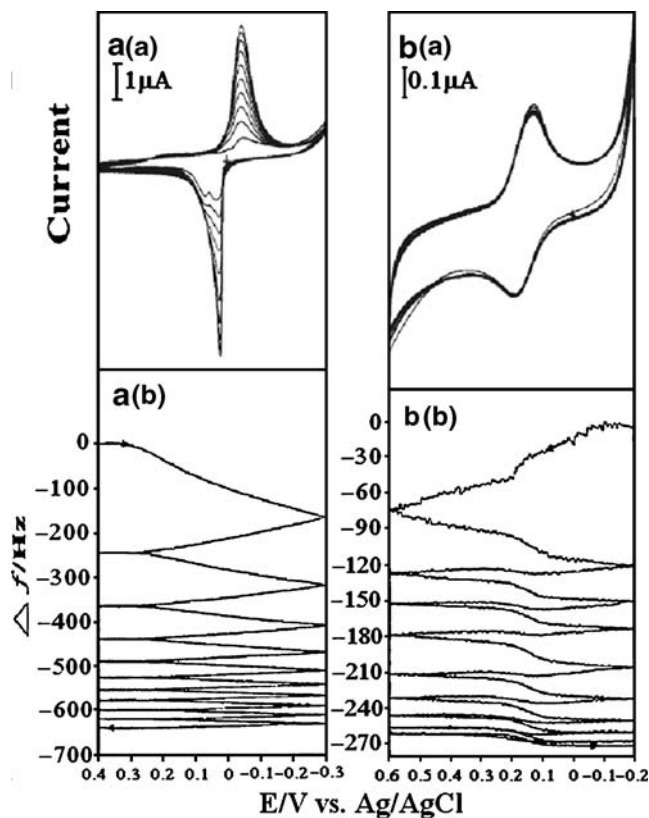


Fig. 9 **a**: Consecutive voltammograms obtained with DDAB film-modified gold electrode in pH 6.5 phosphate buffer solution containing $1 \times 10^{-4} \text{ M Fe}(\text{CN})_6^{3-}$. Scan rate = 0.05 V s^{-1} ; **b**: Respective EQCM frequency changes; **c**: Consecutive voltammograms obtained with PDDAC film-modified gold electrode in pH 6.5 phosphate buffer solution containing $1 \times 10^{-4} \text{ M Fe}(\text{CN})_6^{3-}$; Scan rate = 0.05 V s^{-1} ; **d**: Respective EQCM frequency changes

Hybrid film-coated electrodes showed stable and reversible voltammetric responses. However, the voltammetric features such as shape, peak potentials depend on coating composition. For example, the formal potential (E^{0r}) of redox couples in the coating is shifted to more negative potential than those obtained at bare electrode as mentioned in the previous sections. The E^{0r} values of $\text{Fe}(\text{CN})_6^{3-/4-}$ and $\text{Ru}(\text{CN})_6^{3-/4-}$ redox couples on unmodified and in hybrid as well as the potential shift are given in Table 1. The potential shift is more in the case of DDAB film than that of PDDAC film and can be interpreted as that DDAB film stabilizes the oxidized form more efficiently than PDDAC.

The stability of hybrid coatings derived from DDAB and PDDAC was evaluated by cycling the modified electrodes in dopant-free buffer at different scan rates, as discussed previously. The peak currents of redox couples present in the coatings increased with increasing scan rates. In addition, the stability of modified electrode was also tested by scanning the electrode potential continuously in pure supporting electrolyte at a fixed scan rate. The peak current

Table 1 The formal potentials, of $\text{Fe}(\text{CN})_6^{3-/4-}$ and $\text{Ru}(\text{CN})_6^{3-/4-}$ redox couples in DDAB and PDDAC coatings and at bare electrode, calculated from the cyclic voltammograms recorded in pH 6.5 aqueous solution

Redox couple and its environment	Formal potentials (E°)/V	$^a \Delta E^\circ$ /V
$\text{Fe}(\text{CN})_6^{3-/4-}$ /DDAB	0.03	0.19
$\text{Ru}(\text{CN})_6^{3-/4-}$ /DDAB	0.56	0.18
$\text{Fe}(\text{CN})_6^{3-/4-}$ /PDDAC	0.17	0.05
$\text{Ru}(\text{CN})_6^{3-/4-}$ /PDDAC	0.68	0.06
$\text{Fe}(\text{CN})_6^{3-/4-}$ (aq)	0.22	–
$\text{Ru}(\text{CN})_6^{3-/4-}$ (aq)	0.74	–

^a Differences in the formal potentials measured at modified electrode and on bare electrode

of hybrid film-modified electrode was monitored. After 50 cycles, the decrease in peak current of hybrid coatings was negligible, which indicates that the present modified electrode was relatively stable.

Electrocatalytic behavior of PDDAC-based hybrid coatings

The electrocatalytic behavior of hybrid coatings derived from PDDAC was investigated towards reduction of SO_5^{2-} and $\text{S}_2\text{O}_8^{2-}$ and oxidation of SO_3^{2-} using cyclic voltammetry.

Mediated reduction of SO_5^{2-} and $\text{S}_2\text{O}_8^{2-}$

Figure 10a and b show cyclic voltammograms of hybrid film coated electrode in a pH 2 aqueous solution (curve a) and in the presence of different concentrations (curve b–d) of SO_5^{2-} and $\text{S}_2\text{O}_8^{2-}$. Curve a' represents reduction of SO_5^{2-} and $\text{S}_2\text{O}_8^{2-}$ on bare electrode. As shown in the figures, there is no detectable current for direct reduction of both analytes on unmodified electrode. On the other hand, cathodic peak current of hybrid film around 0.17 V (vs. Ag|AgCl) corresponding to $\text{Fe}(\text{CN})_6^{3-/4-}$ redox couple increased noticeably, while anodic peak current decreased as concentration of SO_5^{2-} and $\text{S}_2\text{O}_8^{2-}$ increased. At the same time, the peak currents of $\text{Ru}(\text{CN})_6^{3-/4-}$ redox couple was remained unchanged. The results suggested that electrochemically generated $\text{Fe}(\text{CN})_6^{4-}$ ions mediate the reduction of SO_5^{2-} and $\text{S}_2\text{O}_8^{2-}$.

Mediated oxidation of SO_3^{2-}

Figure 10c shows cyclic voltammetric responses of SO_3^{2-} on PDDAC-based hybrid film coated electrode and bare glassy carbon electrode (GCE) in an aqueous solution of pH 2. In Fig. 10c, curve a represents response of modified electrode in the absence of SO_3^{2-} ions. Firstly, compared to

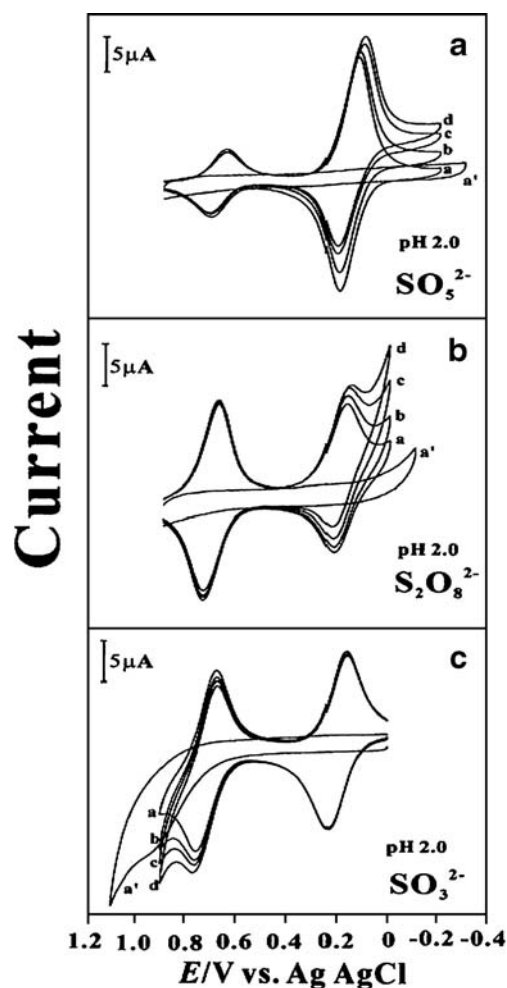


Fig. 10 Cyclic voltammograms of $\text{Fe}(\text{CN})_6^{3-}$ as well as $\text{Ru}(\text{CN})_6^{4-}$ simultaneously doped PDDAC film-modified GCE in a pH 2 aqueous solution containing different concentrations of: **a** SO_5^{2-} (a 0, b 1×10^{-4} , c 2×10^{-4} , and d 3×10^{-4} M); **b** $\text{S}_2\text{O}_8^{2-}$ (a 0, b 1×10^{-4} , c 3×10^{-4} , and d 5×10^{-4} M); **c** SO_3^{2-} (a 0, b 1×10^{-4} , and d 2×10^{-4} M). Curve a' represents the response of sulfur oxoanions. Scan rate = 0.1 V s^{-1}

unmodified electrode (curve a'), the oxidation peak potential of SO_3^{2-} ions at modified electrode shifted toward negative side. Secondly, the anodic peak current of modified electrode at 0.7 V increased with increasing concentration of SO_3^{2-} ions. Thirdly, the peak currents of $\text{Fe}(\text{CN})_6^{3-/4-}$ redox couple was remained unaffected.

Table 2 The electrocatalytic behavior of PDDAC-based hybrid coatings

Substrate	Electrocatalytic peak potential/V	Redox couple responsible for the electrocatalytic mediation	Electrocatalytic reaction type
SO_3^{2-}	0.75	$\text{Ru}(\text{CN})_6^{4-/3-}$	Oxidation
SO_5^{2-}	0.08	$\text{Fe}(\text{CN})_6^{3-/4-}$	Reduction
$\text{S}_2\text{O}_8^{2-}$	0.16	$\text{Fe}(\text{CN})_6^{3-/4-}$	Reduction

Collectively, these observations suggest that electrostatically held $\text{Ru}(\text{CN})_6^{3-/4-}$ redox couple in PDDAC hybrid film was responsible for the enhanced oxidation current, i.e., electrochemically generated $\text{Ru}(\text{CN})_6^{3-}$ ions mediate the oxidation of SO_3^{2-} ions.

The above mediated electrochemical reactions demonstrate the advantages of PDDAC-based hybrid coatings. This kind of coating could be used to mediate both oxidation and reduction reactions, i.e., the same modified electrode could be used to determine different analytes. The electrocatalytic reactions of sulfur oxoanions at PDDAC hybrid coatings are summarized in Table 2.

Conclusions

Electrochemically active hybrid coatings were obtained by cycling the cationic coating-covered electrode repetitively in an aqueous solution containing equimolar concentrations of $\text{Fe}(\text{CN})_6^{3-}$ and $\text{Ru}(\text{CN})_6^{4-}$ anions. Modified electrodes exhibited two redox couples corresponding to $\text{Fe}(\text{CN})_6^{3-/4-}$ and $\text{Ru}(\text{CN})_6^{4-/3-}$ redox transitions. In the film, both anions showed voltammetric characteristics of thin-layer electrochemistry. In situ EQCM experiments indicate that DDAB film could extract larger amount of $\text{Fe}(\text{CN})_6^{3-}$ anions compared to PDDAC coating under similar experimental conditions. The shift in formal potentials of redox couples confined to film towards negative potentials revealed that the environment in the film was different from that of aqueous solution. The shift was about three times higher in DDAB film than that in PDDAC coating. Finally, the electrocatalytic behavior of PDDAC-based hybrid film was tested toward sulfur oxoanions. Same modified electrode could be used to mediate both oxidation and reduction reactions. The response of modified electrodes could be detectable for a reasonable period.

Acknowledgements This work was financially supported by the National Science Council of Taiwan (ROC).

References

1. Snell KD, Keenan AG (1979) *Chem Soc Rev* 8:259
2. Diaz AF, Logan JA (1980) *J Electroanal Chem* 111:111
3. Murray RW (1983) Chemically modified electrodes. In: Bard AJ (ed) *Electroanalytical chemistry*, vol 13. Marcel Dekker, NY, p 191
4. Murray RW (1992) Molecular design of electrode surfaces. *Techniques of chemistry series*, vol XXII. Wiley, New York
5. Lyons MEG (1996) *Electroactive polymers electrochemistry*, part 2. Plenum, New York
6. Rusling JF, Hu N, Zhang H, Miaw CL, Couture E (1992) In: Mackay RA, Texter J (eds) *Electrochemistry in Colloids and Dispersions*. VCH, New York, p 303
7. Finklea HO (1996) Electrochemistry of organized monolayers of thiols and related molecules on electrodes. In: Bard AJ, Rubinstein I (eds) *Electroanalytical Chemistry*, vol.19. Marcel Dekker, New York, p 109
8. Rusling JF (1998) *Acc Chem Res* 31:363
9. Oyama N, Anson FC (1980) *J Electrochem Soc* 127:247
10. Hamachi I, Noda S, Kunitake T (1990) *J Am Chem Soc* 112:6744
11. Hamachi I, Noda S, Kunitake T (1991) *J Am Chem Soc* 113:9625
12. Iwunze MO, Sucheta A, Rusling JF (1990) *Anal Chem* 62:644
13. Rusling JF, Nassar AF (1993) *J Am Chem Soc* 115:11891
14. Rusling JF, Nassar AF (1994) *Langmuir* 10:2800
15. Nassar AF, Willis WS, Rusling JF (1995) *Anal Chem* 67:2386
16. Onuoha AC, Rusling JF (1995) *Langmuir* 11:3296
17. Nassar AF, Zhang Z, Hu N, Rusling JF, Kumosinski TF (1997) *J Phys Chem* 101:2224
18. Ciureanu M, Goldstein S, Mateescu MA (1998) *J Electrochem Soc* 145:533
19. Nassar AF, Narikiyo V, Sagara P, Nakashima N, Rusling JF (1995) *J Chem Soc Faraday Trans* 91:1775
20. Huang Q, Lu Z, Rusling JF (1996) *Langmuir* 12:5472
21. Hu N, Rusling JF (1997) *Langmuir* 13:4119
22. DeCastro ES, Huber EW, Villaroel D, Galiatsatos C, Mark JE, Heineman WR, Murray PT (1987) *Anal Chem* 59:134
23. Huber EW, Heineman WR (1988) *Anal Chem* 60:2467
24. Maizels M, Heineman WR, Seliskar CJ (2000) *Electroanalysis* 12:241
25. J Rusling JF, Zhang H (1991) *Langmuir* 7:1791
26. Oyama N, Shimomura T, Shigehara K, Anson FC (1980) *J Electroanal Chem* 112:271
27. Kuo KN, Murray RW (1982) *J Electroanal Chem* 131:37
28. Braun H, Storck W, Doblhofer K (1983) *J Electrochem Soc* 130:807
29. Petit-Dominguez MD, Shen H, Heineman WR, Seliskar CJ (1997) *Anal Chem* 69:703